Simulated Performance of the FiberGLAST Gamma-Ray Telescope Concept

R.M. Kippen[1], K. Arisaka[2], M. Atac[2], W.R. Binns[3], J.H. Buckley[3], M.L. Cherry[4], M.J. Christl[5], D. Cline[2], P. Dowkontt[3], J.W. Epstein[3], G.J. Fishman[5], T.G. Guzik[4], P.L. Hink[3], M.H. Israel[3], S.C. Kappadath[4], G.R. Karr[1], J. Macri[6], R.S. Mallozzi[1], M.L. McConnell[6], Y. Pischalnikov[2], W.S. Paciesas[1], T.A. Parnell[1], G.N. Pendleton[1], S. Phengchamnan[1], G.A. Richardson[1], K. Rielage[3], J.M. Ryan[6], J.G. Stacy[4,7], T.O. Tümer[8], D.B. Wallace[1] and R.B. Wilson[5]

[1]*Univ. of Alabama in Huntsville, Huntsville, Al 35899, USA*
[2]*Dept. of Physics and Astronomy, University of California, Los Angeles, CA 90095, USA*
[3]*Dept. of Physics & McDonnell Cntr. for Space Sciences, Washington Univ., St. Louis, MO 63130, USA*
[4]*Dept. of Physics, Louisiana State Univ., Baton Rouge, LA 70803, USA*
[5]*NASA/Marshall Space Flight Center, Huntsville, Al 35812, USA*
[6]*Space Science Center, Univ. of New Hampshire, Durham, NH 03824, USA*
[7]*Southern Univ., Baton Rouge, LA 70813, USA*
[8]*Inst. of Geophysics & Planetary Physics, Univ. of California, Riverside, CA 92521, USA*

Abstract

FiberGLAST is one of two main-instrument concepts under study for NASA's Gamma-ray Large Area Space Telescope (GLAST) mission. It uses a large volume of scintillating fiber detectors to image gamma-ray induced showers from 10 MeV to 300 GeV over a wide field-of-view. We present an overview of this concept and report results from simulation studies. Given the expected performance of individual detector elements, the simulations are used to investigate the performance characteristics of the baseline instrument configuration and to develop appropriate triggering and event reconstruction algorithms. The simulation results indicate that *FiberGLAST* can exceed the science performance requirements of GLAST, particularly in terms of sensitivity and field-of-view.

1 Introduction:

The past two decades have been an era of great discovery in the field of gamma-ray astronomy, leading to enhanced knowledge of the most energetic objects and phenomena in the Universe. Although theory has played an important role, the progression of knowledge has been more closely tied to the development and operation of new observational instrumentation. For instance, at energies >50 MeV, the Energetic Gamma Ray Experiment Telescope (EGRET; Thompson *et al.* 1993) on the Compton Observatory has provided comprehensive observations of the entire sky. In the process, EGRET has led to the discovery of an unexpected class of gamma-ray emitting galaxies (blazars), several new gamma-ray pulsars, GeV emission from gamma-ray bursts, particle acceleration in solar flares lasting several hours, 170 unidentified sources, and unprecedented characterization of Galactic and extragalactic diffuse emission (Hartman *et al.* 1999). After more than 8 years of operation, EGRET is facing the end of its remarkable lifetime, and we must look forward to the next generation of higher sensitivity observations for further progress.

The value of a successor to EGRET has been recognized by the scientific community and NASA in their support of the Gamma Ray Large Area Space Telescope (GLAST) mission concept. The GLAST mission is now nearing the end of a technology development phase, wherein two instrument design concepts are being studied: one based on scintillating fiber detectors, and another based on a combination of silicon strip and CsI(Tl) detectors. A key element in the study phase is the development of detailed Monte Carlo simulations that can probe instrument performance given the expected performance of individual detector elements. In this paper, we describe preliminary results from the simulation system developed to study the

scintillating fiber based telescope concept, *FiberGLAST*.

2 *FiberGLAST* Simulation System:

The *FiberGLAST* baseline instrument design is described elsewhere in these proceedings (Rielage et al. 1999). Briefly, the instrument consists of a *tracker* whose primary function is to measure the direction of an incident photon, a *calorimeter* that helps to measure the photon energy, and an *anti-coincidence* (AC) system that distinguishes incident photons from charged particles. The tracker and calorimeter are stacks of 130 cm $\times$ 130 cm planar scintillating fiber detector arrays (0.75 mm square fibers), interspersed with high-Z material (total of 1.8 radiation lengths in the tracker and 5.1 radiation lengths in the calorimeter). The entire active volume is surrounded by a hodoscopic array of plastic scintillator panels that comprise the AC system. As a photon enters the instrument, it is converted in the high-Z material into an e^+e^- pair, and the ensuing electromagnetic cascade development is imaged in three dimensions by the scintillating fiber arrays. The fiber images are used to reconstruct the direction and energy of the photon. The accuracy and efficiency of this process depends on a complex series of statistical and systematic terms, including those inherent to the physics of particle interactions (e.g., pair production, multiple electron scattering, etc.), individual measurement errors, and the details of the reconstruction technique. Monte Carlo particle transport simulation provides an invaluable tool to study this complexity.

The *FiberGLAST* simulation system is composed of four major parts. At the first level, the GEANT Monte Carlo transport system is used to propagate particles through a model of the instrument mass distribution, accumulating energy deposits and interaction locations in the process. The simulation mass model incorporates many fine details of the instrument, including individual scintillating fibers (with passive cladding material), individual AC detector elements, and the passive materials used for structural support, readout hardware, electronics, etc. The second part incorporates the measured performance of the individual detector elements, such as the fiber and AC detection efficiencies (see Rielage *et al.* 1999). In the third part, simulated event fiber and AC data are passed to a sub-system that incorporates hardware and software triggering and background rejection algorithms. Finally, data from the triggered events are processed by a series of algorithms that reconstruct the photon direction and energy. The fully reconstructed event parameters determine the scientific performance of the instrument, such as angular resolution, energy resolution and effective area. The triggering and reconstruction techniques are thus crucial factors affecting instrument performance. Below, we briefly describe these algorithms.

2.1 Trigger and Background Rejection: *FiberGLAST's* large active volume and great number of data channels (>437,000 fibers) make efficient self-triggering a crucial requirement. Furthermore, the large background of cosmic rays requires fast and effective discrimination of photons from charged particles. Using simulation data, we have developed a three-level trigger scheme to address these requirements. The lowest level (L0), uses coarsely grouped fiber data to identify (within a coincidence window of ~1 μs) those events that appear to have an e^+e^- conversion (two particle tracks that span several detector layers). The next level (L1) uses this coarse group data, combined with AC data, to perform a fast rejection of ~95% of charged particles, while retaining ~92% of photons. The last level (L2) acquires individual fiber data to perform more efficient (~99%) background rejection, and to reject Earth albedo photons. All of this processing must be done on-board the spacecraft so as to avoid overwhelming the telemetry system. A more refined background rejection algorithm is applied for science analysis on the ground, but the efficiency losses from on-board processing cannot be recovered. It is thus important for the on-board trigger to retain as many gamma-ray events as is practical.

2.2 Event Reconstruction: Reconstructing the photon direction and energy from a series of secondary particle track measurements is a complex problem. To be effective, the reconstruction algorithm must account for a host of concerns, including track measurement uncertainty (i.e., the 0.75 mm fiber width), the possibility of skipped points due to non-ideal fiber detection efficiency, statistical dispersion due to multiple scattering, and secondary particles that escape the instrument. Our technique was developed over the

course of several years' analysis of simulation data (Pendleton *et al.* 1997, 1998). The basic tracker algorithm proceeds as follows. First, a moments-based analysis determines the rough direction in each orthogonal projection, and computes several measures of dispersion along the length of the event. Second, the moments data are used to identify the incident end of the track, and a more refined search identifies the pair-conversion vertex point common to both projections. Third, starting at the vertex, an iterative search is used to assign points to independent tracks, allowing for some detection inefficiency and accumulating parameters that describe the track dispersion. The next task is to linearly fit the tracks nearest the vertex, being careful not to include track-points that disperse widely from the main path. Finally, the fits to individual tracks in each projection are combined (via weighting parameters related to track dispersion and length) to determine the incident direction and its uncertainty.

The photon energy is reconstructed using information about the position of each fiber hit in the tracker and calorimeter, along with pulse-height data from the calorimeter. At energies <1 GeV, techniques using linear combinations of the number of tracker and calorimeter fiber hits yield reasonable estimates. Above ~1 GeV, the calorimeter pulse-height information must be taken into account, and the data must be adjusted to reflect the differential cascade development, since a considerable amount of energy can escape the system. For events that miss the calorimeter, the energy can be determined (although less accurately) by the kinematics of the shower development.
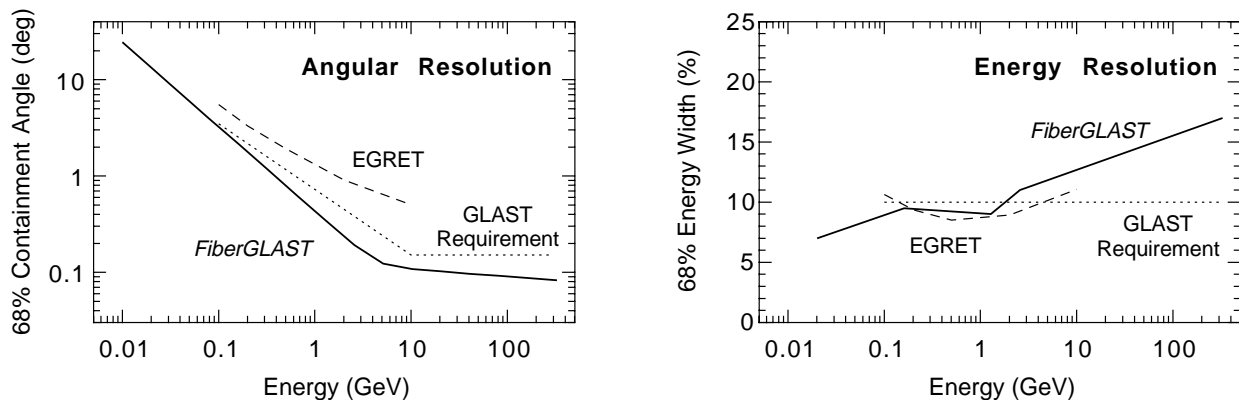

Figure 1: Simulated on-axis angular and energy resolution as a function of photon energy using preliminary event reconstruction algorithms.

3   Performance Results:

The simulation system described above has been used to generate a large database for many different incident gamma-ray directions and energies. Below, we describe instrument performance parameters derived from a subset of this database using preliminary versions of the trigger and reconstruction algorithms. These parameters are compared to those of EGRET (Thompson *et al.* 1993) and to the GLAST mission requirements (as stated in the GLAST Science Requirements Document).

Figure 1 shows the expected *FiberGLAST* angular and energy resolution at normal incidence. The angular resolution improves greatly with increasing energy up to a few GeV due to the statistical effects of dispersion from multiple scattering. At higher energies, these effects become insignificant, and the angular resolution is dominated by the detector plane spacing, fiber position uncertainty, and fluctuations in the physical e^+e^- pair opening angle. The energy resolution is a relatively weak function of energy, but is composed of two components divided at ~1 GeV as discussed above. It is important to note that angular and energy resolution are degraded for off-axis photons. The angular resolution follows a ~sec(θ) relation due to the increased path-length of conversion material, whereas the energy resolution dependence on incidence angle is more complicated. However, even if the incident photon does not hit the calorimeter at all, its energy can still be reconstructed to within ~20-80% (depending on energy) using the shower

development information measured in the tracker. Such "wide-field" photons are valuable for studies that do not depend strongly on angular/energy resolution, such as monitoring emission from variable objects like blazars, and serendipitous discovery of transient sources like gamma-ray bursts, blazars, and solar flares.
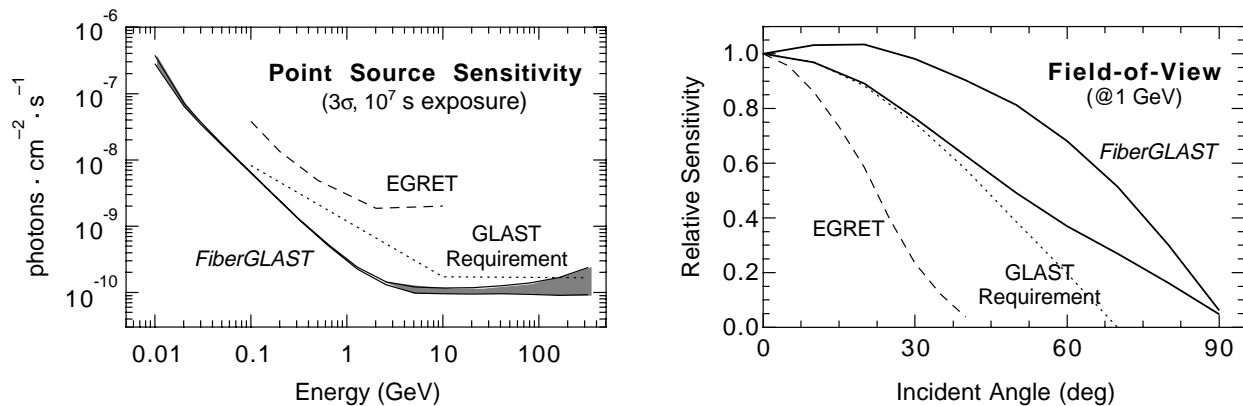

Figure 2: (*left*) On-axis point-source sensitivity well off the Galactic plane. The shaded region indicates the uncertainty in preliminary trigger and background rejection algorithms. (*right*) Relative point-source sensitivity as a function of viewing angle at 1 GeV (results are similar at other energies) for the same Galactic location. The lower solid curve excludes "wide-field" events that do not interact significantly in the calorimeter (and thus have degraded energy resolution), while the upper solid curve includes all events.

The most important factors determining instrument sensitivity in the high-energy gamma-ray regime are effective detection area and angular resolution. Angular resolution is important to be able to distinguish source photons from diffuse Galactic (Bertsch *et al.* 1993) and extragalactic (Sreekumar *et al.* 1998) emission. Shown in Figure 2 is the on-axis and off-axis point-source sensitivity for an observation at 60° Galactic latitude, where Galactic diffuse emission is small compared to the cosmic diffuse flux. These curves incorporate the efficiency losses expected at each processing step. The sensitivity dependence on energy closely follows the angular resolution curve of Figure 1, with some modification in the threshold energy range <50 MeV. The advantage of wide-field photons is apparent—yielding a significant addition to the field-of-view.

4 Conclusions:

The preliminary simulated performance estimates given in this paper demonstrate that *FiberGLAST* could be a capable successor to EGRET—offering significantly improved angular resolution, field-of-view, and sensitivity. In addition to meeting the basic GLAST mission performance requirements, *FiberGLAST* offers enhanced capability for certain scientific objectives with its "wide-field" photon mode. It should be noted that some improvement in the final performance estimates is expected when the triggering and event reconstruction algorithms are fully optimized.

References

Bertsch, D.L., *et al.* 1993, ApJ 416, 587
Hartman, R.C., *et al.* 1999, ApJS in press
Pendleton, G.N., *et al.* 1998, SPIE Proc. 3446, 247
Pendleton, G.N., *et al.* 1997, SPIE Proc. 2806, 164
Rielage, K., *et al.* 1999, Proc. 26th ICRC (these proceedings), OG 4.2.21
Sreekumar, P., *et al.* 1998, ApJ 494, 523
Thompson, D.J., *et al.* 1993, ApJS 86, 629